

Synergistic roles of Mdm2 and Mdm4 for p53 inhibition in central nervous system development

Shunbin Xiong*, Carolyn S. Van Pelt†, Ana C. Elizondo-Fraire*, Geng Liu*, and Guillermina Lozano**

Departments of *Molecular Genetics and †Veterinary Medicine and Surgery, University of Texas M. D. Anderson Cancer Center, 1515 Holcombe Boulevard, Houston, TX 77030

Edited by Peter K. Vogt, The Scripps Research Institute, La Jolla, CA, and approved December 21, 2005 (received for review September 28, 2005)

Loss of *Mdm2* or *Mdm4* leads to embryo lethal phenotypes that are p53-dependent. To determine whether Mdm2 and Mdm4 inhibit p53 function redundantly in a more restricted cell type, conditional alleles were crossed to a neuronal specific Cre transgene to delete *Mdm2* and *Mdm4* in the CNS. Mice lacking *Mdm2* in the CNS developed hydranencephaly at embryonic day 12.5 due to apoptosis, whereas *Mdm4* deletion showed a proencephaly phenotype at embryonic day 17.5 because of cell cycle arrest and apoptosis. The deletion of both genes, strikingly, contributed to an even earlier and more severe CNS phenotype. Additionally, *Mdm2* and *Mdm4* had a gene dosage effect, because loss of three of the four *Mdm* alleles also showed a more accelerated CNS phenotype than deletion of either gene alone. All phenotypes were rescued by deletion of *p53*. Thus, these *in vivo* data demonstrate the importance of Mdm4 independent of Mdm2 in inhibition of p53.

apoptosis | cell cycle arrest | conditional alleles

The importance of the p53 tumor suppressor is highlighted by the observation that proliferating tumor cells have devised multiple mechanisms to disrupt its activity. Diminished p53 activity allows increased proliferation and inhibition of apoptosis, providing advantageous signals for tumor cell survival (1). By far the most common means of disrupting p53 is through mutation of the gene itself (2). Recently, however, several negative regulators of p53 have been discovered (3–6). Two of these, Mdm2 and Mdm4, are overexpressed in many tumors of diverse origin (7–9). Thus, increased levels of p53 inhibitors in tumor cells yield the same end result, loss of p53 function.

Mouse models have provided invaluable insight into the importance of Mdm2 and Mdm4 as negative regulators of p53 activity. Loss of either *Mdm2* or *Mdm4* leads to embryo lethal phenotypes that are completely rescued by concomitant deletion of *p53*, emphasizing the importance of these negative regulators for p53 activity (10–14). Loss of *Mdm2* leads to cell death by a p53-dependent apoptotic mechanism, whereas deletion of *Mdm4* leads to cell cycle arrest sometimes associated with apoptosis (12, 14, 15). Loss of cell viability in these examples occurs at different developmental stages, at implantation for *Mdm2*-null embryos, and at gastrulation for *Mdm4*-null embryos. The early embryo lethal phenotypes of *Mdm2*- and *Mdm4*-null embryos preclude analyses of the function of these proteins in a spatial and temporal specific manner.

Clearly, Mdm2 and Mdm4 are potent p53 inhibitors, but their relationship is more complex. Mdm2 is an ubiquitin ligase that catalyzes ubiquitination of p53 and itself (16–19). Mdm4 inhibits p53 by binding and masking the transcriptional activation domain, but it cannot ubiquitinate p53 (4, 20–22). However, both Mdm2 and Mdm4 bind the same p53 domain with similar affinities, implying a potential competition for inhibition of p53 activity (23). Additionally, interactions between Mdm2 and Mdm4 have been detected through their respective RING domains (24, 25). The dependency of Mdm2 and Mdm4 on each other for inhibition of p53 activity *in vivo* has not been examined. To address these questions, we have generated *Mdm2* and *Mdm4* conditional alleles (26, 27).

To examine the importance of Mdm2 and Mdm4 and their redundancy in a single cell type, we chose to delete both in the CNS for several reasons. First, upon γ radiation of embryos, the CNS shows a strong p53-dependent apoptotic response (28). Additionally, the CNS consists of a proliferating layer of cells that migrate as they differentiate. Proliferating cells are also present in different locations within the ventricular zone, depending on the stage of the cell cycle. Postmitotic cells exit the ventricular zone and migrate outward to form differentiated layers (29, 30). Thus, the role of Mdm2 and Mdm4 in proliferating and differentiated cells could be examined at the same time. Last, *Mdm2* and *Mdm4* are expressed in the early CNS (14, 31, 32). We therefore used the *Nestin-Cre* (*Nes-Cre*) transgenic mice that contain the *Nestin* enhancer and express *Cre* exclusively in the CNS (33) and asked whether Mdm2 and Mdm4 have a role in the inhibition of p53 activity in CNS development.

Results

Loss of Mdm2 or Mdm4 in the CNS Caused Neonatal Lethality. The generation of conditional alleles for *Mdm2* and *Mdm4* indicates that Cre-mediated recombination results in loss-of-function alleles and phenotypes identical to the original deletions (26, 27). Both *Mdm2* and *Mdm4* conditional alleles were mated to the neuronal specific *Nes-Cre* transgenic mice that contain the *Nestin* enhancer and express *Cre* exclusively in the CNS (33). To examine the specificity of *Cre* expression in *Nes-Cre* transgenic mice, we also crossed *Mdm2* conditional *Nes-Cre* mice to the *ROSA26* reporter mice (34). Cre-specific recombination at the *ROSA26* locus allows expression of β -galactosidase. Robust and specific LacZ staining in the CNS was observed beginning at embryonic day (E)10.5, consistent with published data (33). At later stages, E12.5 (Fig. 1A) and E14.5 (data not shown), LacZ staining remained specific to the CNS.

To determine whether *Mdm2* is required during development of the CNS, we crossed *Mdm2^{FM/FM}* mice (containing the *Mdm2* conditional allele) to *Mdm2^{FM/+} Nes-Cre* mice. Among 44 mice born from this cross, no *Mdm2^{FM/FM} Nes-Cre* mice were obtained at weaning (Table 1). However, on several occasions, pups with abnormal heads were born but died immediately thereafter. We therefore dissected embryos from the above cross. We observed a domed-head phenotype with decreased neuronal tissue throughout the brain compartment and especially in the hind-brain and spinal cord in *Mdm2^{FM/FM} Nes-Cre* embryos (which sometimes also contained the *ROSA26* locus) as early as E12.5 (Fig. 1A). From other crosses, we also generated *Mdm2^{-/FM} Nes-Cre* mice so that recombination from a single *Mdm2* allele would result in complete loss of *Mdm2*. These mice contained the same domed head phenotype and loss of neuronal cells, indi-

Conflict of interest statement: No conflicts declared.

This paper was submitted directly (Track II) to the PNAS office.

Freely available online through the PNAS open access option.

Abbreviations: En, embryonic day *n*; *Nes-Cre*, *Nestin-Cre*.

*To whom correspondence should be addressed. E-mail: gglozano@mdanderson.org.

© 2006 by The National Academy of Sciences of the USA

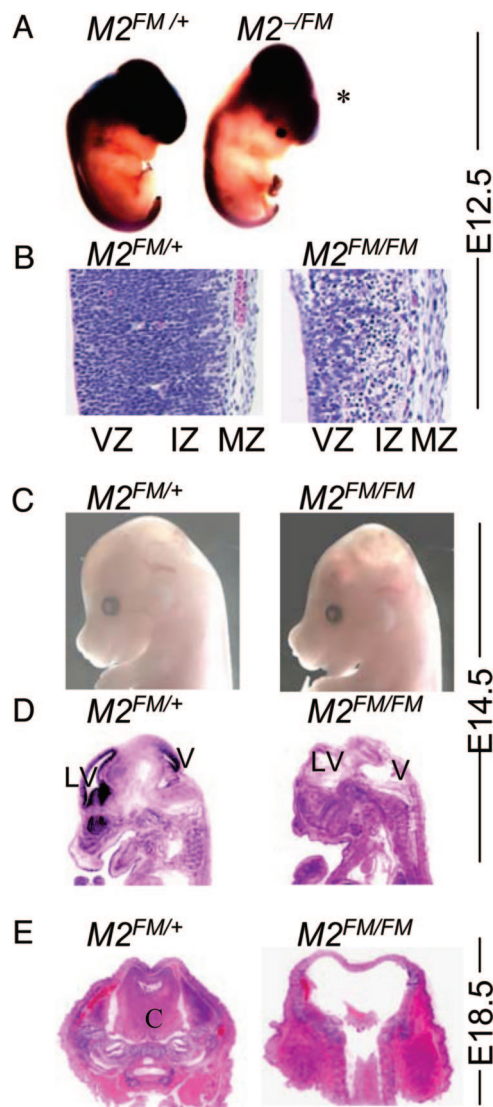


Fig. 1. Hydranencephaly in mice lacking *Mdm2* in the CNS. (A) Whole-mount LacZ staining of E12.5 embryos. (B) Hematoxylin/eosin (H&E)-stained sections of the forebrain at E12.5. (C) Embryos at E14.5. (D) Sagittal sections of embryos stained with H&E at E14.5. (E) Cross sections of E18.5 embryos. All embryos have the *Nes-Cre* transgene. The other alleles are labeled as follows: $M2^{FM/+}$, $M2^{FM/FM}$, $M2^{-IFM}$, $Mdm2^{-IFM}$; VZ, ventricular zone; IZ, intermediate zone; MZ, marginal zone; V, ventricle; LV, lateral ventricle; and C, cortex.

cating the Cre-mediated recombination efficiently deleted both *Mdm2* conditional alleles (data not shown). This phenotype was never observed in mice that had one wild-type *Mdm2* allele and/or *Nes-Cre*. Sections through the embryonic brain revealed that the mutant embryos had much thinner cerebral cortexes at E12.5 (Fig. 1B). At this developmental stage, the cerebral cortex consists of ventricular and intermediate zones. Cells of the intermediate zone had lost their elongated morphology and appeared smaller and disorganized. The marginal zone was not affected in these embryos. At E14.5, all $M2^{FM/FM}$ *Nes-Cre* mutant embryos clearly displayed an obvious domed head with excess cerebrospinal fluid in the brain, characterized as hydranencephaly (Fig. 1C and D). Furthermore, the ventricular zone of CNS in these mutant brains was completely disordered (Fig. 1D). At E18.5, a normal Mendelian ratio of $M2^{FM/FM}$ *Nes-Cre* embryos was still observed (Table 1), even though almost no neuronal tissue was left in the brain (Fig. 1E).

Table 1. Deletion of *Mdm2* (M2) in CNS causes neonatal lethality

Age	Cross: $M2^{FM/FM} \times M2^{FM/+}$ <i>Nes-Cre</i>					
	Phenotypes		Genotypes*			
	Normal	Abnormal	$M2^{FM/+}$	$M2^{FM/FM}$	$M2^{FM/+}$ <i>Nes-Cre</i>	$M2^{FM/FM}$ <i>Nes-Cre</i>
E12.5	36	5	11	10	10	10
E14.5	12	4	4	5	3	4
E18.5	24	10	9	7	8	10
3 weeks	44	0	13	15	16	0

*All genotypes are expected at 25%.

The same strategy was used to generate *Mdm4*-specific deletion in CNS. No $Mdm4^{FX/FX}$ *Nes-Cre* mice were obtained at weaning among 40 mice from a cross between $Mdm4^{FX/FX}$ and $Mdm4^{FX/+}$ *Nes-Cre* mice (Table 2). When the embryos were examined from this cross, the $Mdm4^{FX/FX}$ *Nes-Cre* mice appeared to be normal at E14.5 (data not shown), even though PCR using DNA prepared from the whole embryo head (including some nonneuronal tissue) showed most of the conditional allele recombined at this stage (Fig. 2A). Embryos examined at later stages showed that deletion of *Mdm4* did not cause obvious defects in the mutant embryos until E17.5 (Table 2). At this stage, the mutant embryos exhibited flat heads caused by the presence of a large cavity in the brain, characteristic of a proencephaly phenotype (data not shown). This phenotype was even more pronounced at E18.5 (Fig. 2B and C). Thus, results from deletion of *Mdm2* and *Mdm4* alleles in the CNS clearly demonstrated that *Mdm2* and *Mdm4* were absolutely essential during the development of the CNS. Additionally, loss of the *Mdm2* allele caused an earlier and more severe phenotype than loss of *Mdm4*.

Loss of *Mdm2* or *Mdm4* Induces Aberrant Apoptosis and Cell Proliferation. Loss of *Mdm2* induces p53-dependent apoptosis at E3.5, whereas loss of *Mdm4* causes p53-dependent cell cycle arrest at E7.5 (12, 15). A different allele of *Mdm4* showed a delayed phenotype, with onset of cell cycle arrest and apoptosis in the neuroepithelium at E10.5 (14). We therefore, examined embryos for the mechanism of cell loss. Because *Nes-Cre* transgenic mice showed robust Cre recombinase activity as early as E10.5 (33), we examined whether loss of *Mdm2* caused neuronal progenitor cells to undergo apoptosis or cell cycle arrest in sections of E10.5 embryos. Loss of *Mdm2* induced massive apoptosis in the ventricular zone (Fig. 3A). By contrast, cell proliferation as measured by BrdUrd incorporation was the same between the mutant and the control mice (Fig. 3B). The only difference was that at this developmental stage, the location of BrdUrd-positive cells varied between mutant and control embryos. These data indicated that the hydranencephaly phenotype caused by loss of

Table 2. Deletion of *Mdm4* (M4) in CNS causes neonatal lethality

Age	Cross: $M4^{FX/FX} \times M4^{FX/+}$ <i>Nes-Cre</i>					
	Phenotypes		Genotypes*			
	Normal	Abnormal	$M4^{FX/+}$	$M4^{FX/FX}$	$M4^{FX/+}$ <i>Nes-Cre</i>	$M4^{FX/FX}$ <i>Nes-Cre</i>
E14.5	11	0	3	3	2	3
E17.5	16	2	6	5	5	2
E18.5	18	5	7	5	6	5
3 weeks	40	0	10	15	15	0

*All genotypes are expected at 25%.

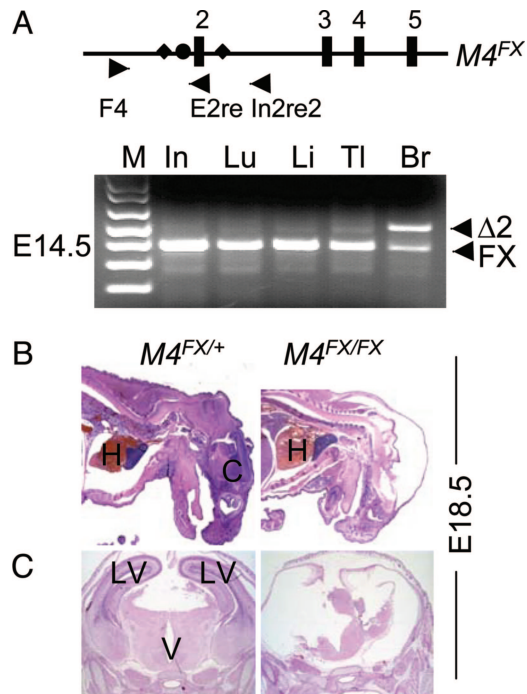


Fig. 2. Proencephaly in mice lacking *Mdm4* in the CNS. (A) Specific recombination of the *Mdm4*^{FX} allele in E14.5 *Mdm4*^{FX/FX} *Nes-Cre* embryos. Numbers label *Mdm4* exons (boxes). The closed circle is an *frt* site, and diamonds are loxP sites. The triangles are PCR primers used for detection of the recombination event. F4 and E2re amplify the *Mdm4* conditional allele. F4 and In2re2 amplify the *Mdm4* allele ($\Delta 2$) after recombination. Hematoxylin/eosin-stained sagittal (B) and coronal (C) sections of embryos at E18.5. All embryos have the *Nes-Cre* transgene. *M4*^{FX/+}, *M4*^{FX/+}, *M4*^{FX/FX}, and *M4*^{FX/FX}; M, 1-kb-plus marker; In, intestine; Lu, Lung; Li, Liver; TI, Tail; Br, Brain; H, Heart; C, cortex; V, ventricle; and LV, lateral ventricle.

Mdm2 was due to increased apoptosis, consistent with previous observations in pluripotent cells from *Mdm2*-null embryos (15).

Because deletion of *Mdm4* in the CNS had a phenotype at E17.5, but *Mdm4* loss was clearly apparent at E14.5, sections from E14.5 embryos were assayed for apoptosis and cell proliferation. Apoptosis was clearly increased in the mutant CNS (Fig. 3C). Additionally, when DNA synthesis was measured, loss of *Mdm4* dramatically decreased BrdUrd staining in the ventricular zone (Fig. 3D). These data suggested that *Mdm4* loss in the CNS actually induced both apoptosis and cell cycle arrest.

Mdm2 mediates p53 degradation through its E3 ubiquitin ligase activity (17). Although *Mdm4* does not degrade p53, it interacts with *Mdm2* to modulate p53 activity (24, 35). Therefore, to determine whether loss of *Mdm2* or *Mdm4* in the CNS caused elevation of p53 protein levels, immunohistochemistry was performed on brain sections from embryos. At E10.5, clear p53 staining was detected in *Mdm2*- but not *Mdm4*-null cells (Fig. 4A and B). Wild-type controls also do not stain with p53 antibodies (data not shown). However, when p53 staining was

Table 3. Deletion of p53 rescues the lethality of *Mdm2* (M2) loss

	Cross: <i>M2</i> ^{+/FM} <i>p53</i> ^{+/-} <i>Nes-Cre</i> × <i>M2</i> ^{FM/FM} <i>p53</i> ^{-/-} genotypes*			
	<i>M2</i> ^{FM/+}	<i>M2</i> ^{FM/FM}	<i>M2</i> ^{FM/+} <i>Nes-Cre</i>	<i>M2</i> ^{FM/FM} <i>Nes-Cre</i>
<i>p53</i> ^{+/-}	5	6	5	0
<i>p53</i> ^{-/-}	7	5	5	4

*All genotypes are expected at the same ratio.

Table 4. Deletion of p53 rescues the lethality of *Mdm4* (M4) loss

	Cross: <i>M4</i> ^{+/FX} <i>p53</i> ^{+/-} <i>Nes-Cre</i> × <i>M4</i> ^{FX/FX} <i>p53</i> ^{-/-} genotypes*			
	<i>M4</i> ^{FX/+}	<i>M4</i> ^{FX/FX}	<i>M4</i> ^{FX/+} <i>Nes-Cre</i>	<i>M4</i> ^{FX/FX} <i>Nes-Cre</i>
<i>p53</i> ^{+/-}	11	15	16	0
<i>p53</i> ^{-/-}	14	11	9	6

*All genotypes are expected at the same ratio.

performed on E14.5 embryos, *Mdm4*-null cells also clearly had high levels of p53 (Fig. 4C). *Mdm2*-null embryos could not be analyzed at this developmental stage because of loss of most neuronal tissue. To further probe the functionality of increased p53 in cells lacking *Mdm4*, sections of embryos were immunostained with an antibody for p21, a p53 target. Again, clearly p21 levels were higher in the ventricular and intermediate zones although some background was visible in normal embryos (Fig. 4D). Western blot analyses of embryos confirmed the increase in p53 and p21 in *Mdm2*- and *Mdm4*-null CNS at E10.5 and E14.5, respectively (Fig. 4E). The increase in p53 levels in *Mdm2*-null embryos could not be quantitated because of the lack of detectable p53 in wild-type embryos at this stage. However, at E14.5, *Mdm4*-null embryos showed a 3- and 10-fold increase in p53 and p21 levels, respectively. Real-time PCR, performed with five different p53 targets, showed that p53 targets were also expressed at higher levels in *Mdm2*- and *Mdm4*-null CNS at these developmental stages (Fig. 4F and G).

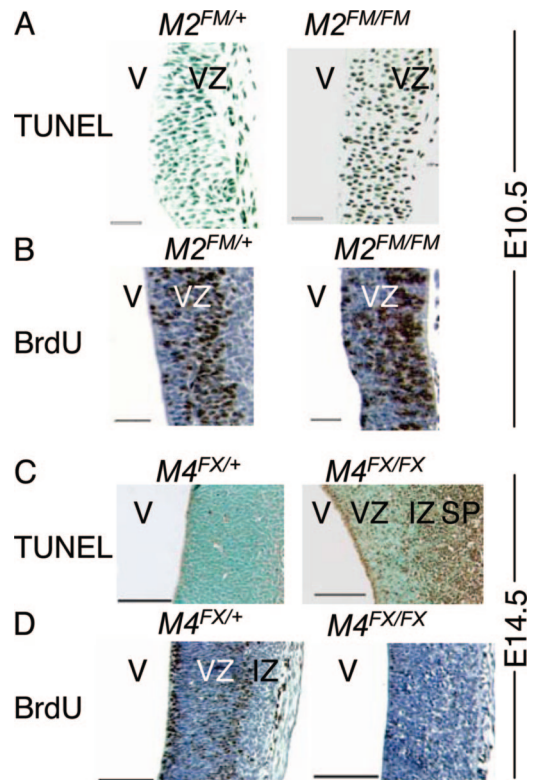


Fig. 3. Apoptosis and proliferation in mice lacking *Mdm2* or *Mdm4* in the forebrain. TUNEL (A and C) and BrdUrd assays (B and D) in the CNS from E10.5 embryonic brains (A and B) from control *Mdm2*^{FM/+} *Nes-Cre* (*M2*^{FM/+}) and mutant *Mdm2*^{FM/FM} *Nes-Cre* (*M2*^{FM/FM}) mice. E14.5 embryonic brains (C and D) from control *Mdm4*^{FX/+} *Nes-Cre* (*M4*^{FX/+}) and mutant *Mdm4*^{FX/FX} *Nes-Cre* (*M4*^{FX/FX}) mice. VZ, ventricular zone; IZ, intermediate zone; SP, subplate; and V, ventricle. (Scale bars, 50 μ m for A and B; 100 μ m for C and D.)

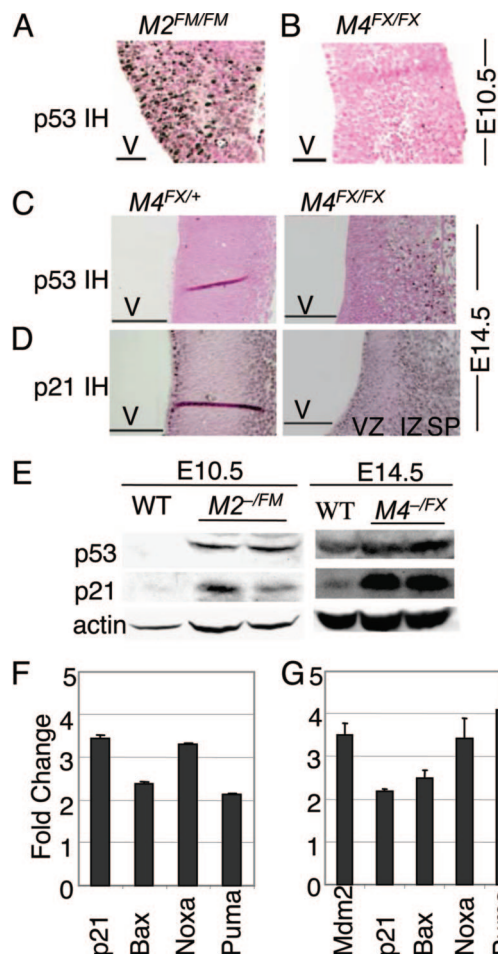


Fig. 4. Loss of *Mdm2* and *Mdm4* caused increased p53 protein levels. p53 immunohistochemical staining of E10.5 (A and B) and E14.5 (C) sections of the forebrain. (D) p21 immunohistochemical staining of E14.5 embryonic brains. (E) Western blot analysis of embryo extracts. Real-time RT-PCR of *Mdm2^{FM/FM} Nes-Cre* (F) and *Mdm4^{FX/FX} Nes-Cre* (G) samples. V, ventricle; VZ, ventricular zone; IZ, intermediate zone; and SP, subplate. (Scale bars, 50 μ m for A and B; 100 μ m for C and D.)

Lethal Phenotypes from Loss of *Mdm2* and *Mdm4* in the CNS Are p53-Dependent. Because *Mdm2* and *Mdm4* negatively regulate p53, and deletion of *Mdm2* and *Mdm4* in the CNS clearly showed elevated p53 activity, we asked whether the phenotypes due to loss of *Mdm2* and *Mdm4* in the CNS were p53-dependent. We therefore generated *Mdm2^{FM/FM} Nes-Cre p53^{-/-}* mice. Remarkably, the *Mdm2^{FM/FM} Nes-Cre p53^{-/-}* mice were born at the correct Mendelian ratio and had no obvious defects (Table 3). The same strategy was used to generate *Mdm4^{FX/FX} Nes-Cre p53^{-/-}* mice. These mice were also alive without apparent defects (Table 4). These data demonstrated that the neuronal defects induced by deletion of *Mdm2* or *Mdm4* were p53-dependent and indicated that *Mdm2* and *Mdm4* are essential negative regulators of p53 in CNS development.

Synergistic Inhibition of p53 by *Mdm2* and *Mdm4*. The relationship between *Mdm2* and *Mdm4* is complex. *Mdm2* loss results in increased p53 stability (36, 37), but *Mdm2* also binds *Mdm4* and decreases stability of *Mdm4* (38, 39). *Mdm4* overexpression stabilizes p53 by inhibiting *Mdm2*-mediated degradation of p53 (20, 22). Modulation of p53 protein levels by *Mdm4* could occur through *Mdm2*. However, whether *Mdm2* and *Mdm4* cooperate or independently regulate p53 is unknown. A requirement for

both proteins in a single cell type has not been examined. Therefore, we generated mice null for both *Mdm2* and *Mdm4* in the CNS by crossing *Mdm2^{+/-} Mdm4 ^{Δ 2/+} Nes-Cre* mice to *Mdm2^{FM/FM} Mdm4^{FX/FX}* mice. In this cross, 50% of the mice will have one conditional and one null allele for *Mdm2* and *Mdm4*. Strikingly, mice lacking *Mdm2* and *Mdm4* in the CNS showed gross abnormalities at E11.5 (Fig. 5 A and B), which was even earlier than the phenotype seen with loss of *Mdm2* at E12.5 (Fig. 1 A and B). In addition, hemorrhaging in the CNS was visible at E11.5, a phenotype not observed in cells lacking either *Mdm2* or *Mdm4* (data not shown). At E13.5, embryos lacking *Mdm2* and *Mdm4* clearly showed a domed-head phenotype with obvious hemorrhaging in the brain (Fig. 5 C and D). These embryos died at E15.5, as measured by absence of movement and pale color, in contrast to loss of *Mdm2* or *Mdm4* alone, which yielded live pups at birth. When crossed to the *ROSA26* reporter strain, *Mdm2^{FM/-} Mdm4^{FX/ Δ 2} Nes-Cre* mice had fewer LacZ-positive cells in the hindbrain and spine than the *Mdm2^{FM/-}* mice, indicating that loss of *Mdm2* and *Mdm4* caused cell depletion earlier than *Mdm2* loss alone (Fig. 5 E and F).

These crosses also produced mice with different combinations of *Mdm2* and *Mdm4* alleles in a *Nes-Cre* background. Mice lacking *Mdm2* coupled with loss of one *Mdm4* allele displayed ventricular defects and hemorrhaging in the CNS at E13.5, phenotypes that were more dramatic than *Mdm2* loss alone (Fig. 5 C–E). Additionally, loss of *Mdm4* with loss of one *Mdm2* allele also had a more severe phenotype than loss of *Mdm4* alone (Fig. 5 C–E). The severity of phenotypes was graded with double null > *Mdm2* null *Mdm4* heterozygous > *Mdm4* null *Mdm2* heterozygous > *Mdm2* null > *Mdm4* null. These data suggest a gene dosage effect of *Mdm2* and *Mdm4* on inhibition of p53 activity. These data indicate that loss of both *Mdm2* and *Mdm4* contributed to a more severe phenotype and imply that *Mdm4* together with *Mdm2* contributed to inhibition of p53 in the same cell type. These observations strongly support the synergistic nature of *Mdm2* and *Mdm4* in the inhibition of p53 activity in the development of the CNS.

The proliferation defects distinguish *Mdm2*- from *Mdm4*-null cells in this and other systems (12, 14, 15, 36). Because *Mdm4* loss but not *Mdm2* loss showed a clear defect in proliferation, we examined embryo sections for cell cycle arrest. Remarkably, although cells lacking *Mdm2* did not show a proliferation defect, cells lacking both *Mdm2* and *Mdm4* showed a clear cell cycle arrest phenotype similar to loss of *Mdm4* alone (Fig. 6A). In addition, cells in embryos lacking both *Mdm2* and *Mdm4* still exhibited apoptosis similar to that of loss of *Mdm2* (Fig. 6B). These data suggest *Mdm4* has a unique function in inhibition of p53-dependent cell cycle arrest, and that it contributes to the overall inhibition of p53 activity independent of *Mdm2*. We also performed immunostaining of p21 in E10.5 embryonic sections and observed that only *Mdm2^{FM/-} Mdm4^{FX/ Δ 2} Nes-Cre* mice had clear p21 expression in the midbrain at this time point, suggesting that loss of *Mdm2* and *Mdm4* activated p53 transcriptional activity even better than loss of *Mdm2* or *Mdm4* alone (Fig. 6C). This observation was supported by real-time RT-PCR of mice lacking *Mdm2*, *Mdm4*, or both genes in the CNS (Fig. 6D). Although increases in all p53 targets analyzed were clear, p21 was the only target that increased additively in mice lacking *Mdm2* and *Mdm4* in the CNS. These data strongly support the cooperative nature of *Mdm2* and *Mdm4* function in inhibition of p53 activity during the development of the CNS. Last, but important, the embryo lethal phenotype of *Mdm2^{FM/-} Mdm4^{FX/ Δ 2} Nes-Cre* mice was completely rescued by deletion of p53.

Discussion

This study makes several observations. The first is that *Mdm2* and *Mdm4* were required for proper development of the CNS.

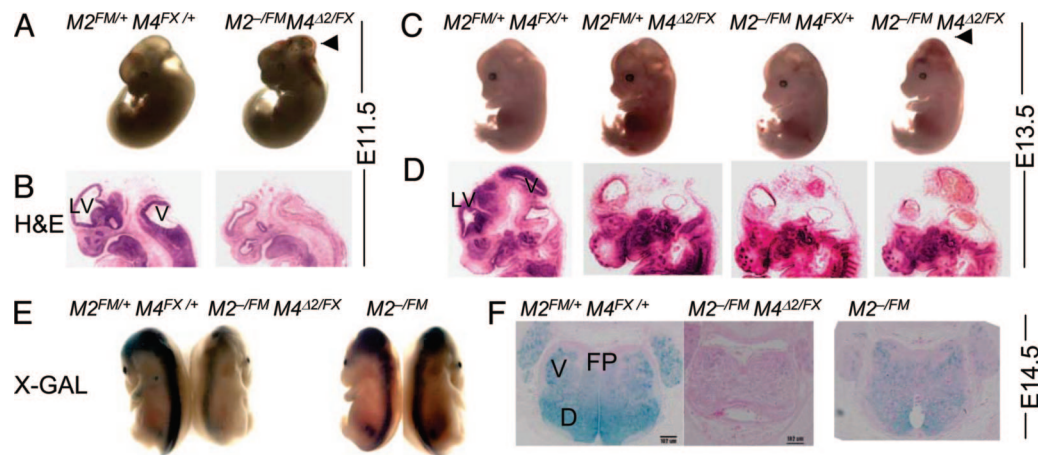


Fig. 5. Loss of *Mdm2* and *Mdm4* in the CNS caused an earlier and more severe phenotype than loss of either gene alone. Embryos and hematoxylin/eosin sections at E11.5 (A and B) and E13.5 (C and D). Arrows indicate hemorrhaging in the brain. Embryos at E14.5 were stained for LacZ and shown as whole embryos (E) and cross sections (F). M2, *Mdm2*; M4, *Mdm4*; D, dorsal; V, ventral; and FP, floor plate.

Loss of *Mdm2* yielded a dramatic phenotype with embryos exhibiting hydranencephaly as early as E12.5, whereas embryos lacking *Mdm4* showed the first signs of gross defects at E17.5. Second, a synergistic effect was visible upon deletion of both *Mdm2* and *Mdm4*. These data provide clear genetic support for independent function of *Mdm4*. Third, all defects are p53-dependent, affirming the important role of these negative regulators on p53 function. Importantly, these embryos were not subject to DNA-damaging agents and thus highlight the role of p53 in normal cell cycling.

Additionally, it is clear that the loss of *Mdm2* results in a p53-dependent apoptotic phenotype in the developing CNS. Embryonic stem cells and mouse embryo fibroblasts also die by initiating apoptosis in the absence of *Mdm2* (15, 36). Thus, no *Mdm2*-null cell is viable unless p53 is absent. In contrast, loss of *Mdm4* yields a cell cycle arrest phenotype that is in some, but not all, cases accompanied by apoptosis (12, 14). This cell cycle arrest phenotype is not seen in *Mdm2*^{-/-} cells regardless of developmental stage and as thus distinguishes *Mdm2*- from *Mdm4*-null cells. Possibly *Mdm2* and *Mdm4* bind different p53 molecules that are posttranslationally modified to regulate apoptosis or cell cycle arrest. The data clearly show a role for *Mdm4* in inhibition of p53, complementing that of *Mdm2*. In line with this thought, loss of one additional *Mdm2* allele in an *Mdm4*-null background showed a more severe phenotype than loss of *Mdm4* alone, and

vice versa, deletion of *Mdm2* and one *Mdm4* allele also showed a more severe phenotype than *Mdm2*-null cells alone. These data indicate that *Mdm2* and *Mdm4* have a gene dosage effect for inhibition of p53 activity, emphasizing that both have important roles in regulating p53. That both apoptosis and cell cycle arrest functions of p53 are important in tumor suppression has already been determined by analysis of a p53 mutant that differentiates between these activities (40).

Two additional negative inhibitors of p53 have been cloned, Pirh2 and Cop1 (5, 6). The importance of these regulators in embryogenesis is unknown, although studies in cells suggest they may cooperate with *Mdm2* in ubiquitinating p53. *Mdm2*, Pirh2, and Cop1 encode E3 ubiquitin ligases that ultimately result in p53 degradation, whereas *Mdm4* does not. Thus, *Mdm4* may fine tune the transcriptional activity of p53. Differences in the mechanisms of p53 inactivation imply exquisite control at all levels. The presence of so many p53 inhibitors emphasizes the importance of monitoring and dampening p53 function, because its activity is so lethal to the cell.

Materials and Methods

Mice. *Nes-Cre* transgene were purchased from The Jackson Laboratory. The *Mdm2* and *Mdm4* conditional alleles (labeled *Mdm2^{FM}* and *Mdm4^{FX}*, respectively) have been described (26, 27). *Mdm4^{Δ2}* represents the recombined *Mdm4^{FX}* allele, which is

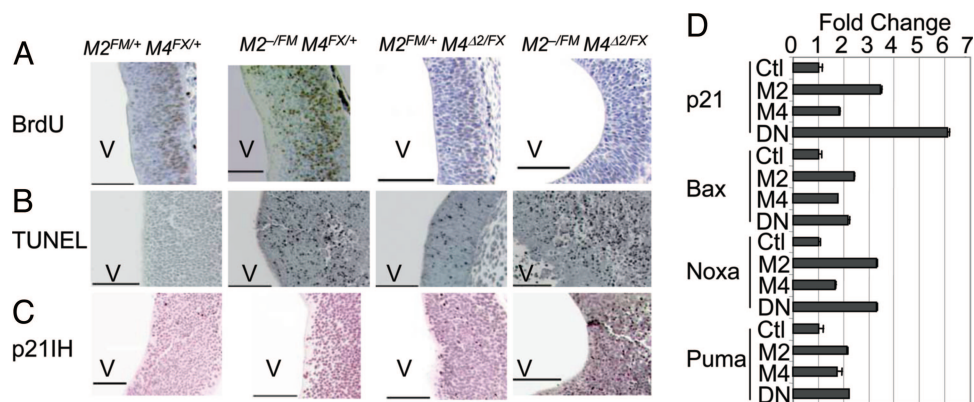


Fig. 6. Apoptosis and cell cycle arrest in embryos lacking *Mdm2* and *Mdm4* in the CNS. BrdUrd (A), TUNEL (B), and p21 immunohistochemical staining (C) of CNS sections of E10.5 embryos. (D) Real-time RT-PCR was performed by using RNA from heads of E10.5 wild-type (Ctl), *Mdm2^{FM/PM} Nes-Cre* (M2), *Mdm4^{FX/FX} Nes-Cre* (M4), and *Mdm2^{FM/PM} Mdm4^{FX/FX} Nes-Cre* (DN) embryos. V, ventricle. (Scale bars, 100 μ m).

due to loss of exon 2, the first coding exon. The *Mdm2*- and *Mdm4*-null alleles have been published (10, 27).

Embryo Analysis. Mouse embryos at different developmental stages were stained for LacZ expression (41). For immunohistochemistry, embryos were fixed overnight in 10% buffered formalin. Immunohistochemistry for p53 or p21 was performed by using the CM5 antibody (Novocastra, Newcastle upon Tyne, U.K.) at a 1:200 dilution or Ab-9 (NeoMarkers, Fremont, CA) at a 1:80 dilution for 2 h at 37°C. ABC and DAB kits from Vector Laboratories were used for subsequent detection. For Western blots, CM5 (Novocastra) and C-19 antibodies (Santa Cruz Biotechnology) were used to detect p53 and p21, respectively. Total RNA was extracted from embryonic brains by using TRIzol reagent (Invitrogen). The first-strand cDNA synthesis kit (Amersham Pharmacia Bioscience) was used for reverse-

transcriptase reactions. Real-time PCR was performed according to the manufacturer's specifications (Applied Biosystems) with previously reported primers (42, 43).

Apoptosis and Proliferation Assays. Apoptosis was assayed in paraffin-embedded sections by using the DNA Fragmentation Detection Kit (Oncogene Research Products, Cambridge, MA). For cell proliferation assays, pregnant females were injected i.p. with 100 $\mu\text{g/g}$ body mass of BrdUrd (Zymed Laboratories) and killed 2 h later. Paraffin embedded sections were analyzed by using the Zymed BrdUrd staining kit.

We thank J. Parant and J. Grier for helpful discussions and Sara Amra for careful preparation of sections. This research was supported by National Institutes of Health Grants CA47296 (to G. Lozano) and CA16672 (to M. D. Anderson Cancer Center).

1. Vousden, K. H. & Prives, C. (2005) *Cell* **120**, 7–10.
2. Hollstein, M., Hergenhahn, M., Yang, Q., Bartsch, H., Wang, Z. Q. & Hainaut, P. (1999) *Mutat. Res.* **431**, 199–209.
3. Momand, J., Zambetti, G. P., Olson, D. C., George, D. & Levine, A. J. (1992) *Cell* **69**, 1237–1245.
4. Shvarts, A., Steegenga, W. T., Riteco, N., van Laar, T., Dekker, P., Bazuine, M., van Ham, R. C., van der Houven van Oordt, W., Hateboer, G., et al. (1996) *EMBO J.* **15**, 5349–5357.
5. Leng, R. P., Lin, Y., Ma, W., Wu, H., Lemmers, B., Chung, S., Parant, J. M., Lozano, G., Hakem, R. & Benchimol, S. (2003) *Cell* **112**, 779–791.
6. Dornan, D., Wertz, I., Shimizu, H., Arnott, D., Frantz, G. D., Dowd, P., O'Rourke, K., Koepfen, H. & Dixit, V. M. (2004) *Nature* **429**, 86–92.
7. Momand, J., Wu, H. H. & Dasgupta, G. (2000) *Gene* **242**, 15–29.
8. Evans, S. C., Viswanathan, M., Grier, J. D., Narayana, M., El-Naggar, A. K. & Lozano, G. (2001) *Oncogene* **20**, 4041–4049.
9. Danovi, D., Meulmeester, E., Pasini, D., Migliorini, D., Capra, M., Frenk, R., de Graaf, P., Francoz, S., Gasparini, P., Gobbi, A., et al. (2004) *Mol. Cell. Biol.* **24**, 5835–5843.
10. Montes de Oca Luna, R., Wagner, D. S. & Lozano, G. (1995) *Nature* **378**, 203–206.
11. Jones, S. N., Roe, A. E., Donehower, L. A. & Bradley, A. (1995) *Nature* **378**, 206–208.
12. Parant, J., Chavez-Reyes, A., Little, N. A., Yan, W., Reinke, V., Jochemsen, A. G. & Lozano, G. (2001) *Nat. Genet.* **29**, 92–95.
13. Finch, R. A., Donoviel, D. B., Potter, D., Shi, M., Fan, A., Freed, D. D., Wang, C. Y., Zambrowicz, B. P., Ramirez-Solis, R., Sands, A. T., et al. (2002) *Cancer Res.* **62**, 3221–3225.
14. Migliorini, D., Denchi, E. L., Danovi, D., Jochemsen, A., Capillo, M., Gobbi, A., Helin, K., Pelicci, P. G. & Marine, J. C. (2002) *Mol. Cell. Biol.* **22**, 5527–5538.
15. Chavez-Reyes, A., Parant, J. M., Amelse, L. L., de Oca Luna, R. M., Korsmeyer, S. J. & Lozano, G. (2003) *Cancer Res.* **63**, 8664–8669.
16. Haupt, Y., Maya, R., Kazaz, A. & Oren, M. (1997) *Nature* **387**, 296–299.
17. Honda, R., Tanaka, H. & Yasuda, H. (1997) *FEBS Lett.* **420**, 25–27.
18. Kubbutat, M. H., Jones, S. N. & Vousden, K. H. (1997) *Nature* **387**, 299–303.
19. Fang, S., Jensen, J. P., Ludwig, R. L., Vousden, K. H. & Weissman, A. M. (2000) *J. Biol. Chem.* **275**, 8945–8951.
20. Jackson, M. W. & Berberich, S. J. (2000) *Mol. Cell. Biol.* **20**, 1001–1007.
21. Little, N. A. & Jochemsen, A. G. (2001) *Oncogene* **20**, 4576–4580.
22. Stad, R., Little, N. A., Xirodimas, D. P., Frenk, R., van der Eb, A. J., Lane, D. P., Saville, M. K. & Jochemsen, A. G. (2001) *EMBO Rep.* **2**, 1029–1034.
23. Bottger, V., Bottger, A., Garcia-Echeverria, C., Ramos, Y. F., van der Eb, A. J., Jochemsen, A. G. & Lane, D. P. (1999) *Oncogene* **18**, 189–199.
24. Sharp, D. A., Kratowicz, S. A., Sank, M. J. & George, D. L. (1999) *J. Biol. Chem.* **274**, 38189–38196.
25. Tanimura, S., Ohtsuka, S., Mitsui, K., Shirouzu, K., Yoshimura, A. & Ohtsubo, M. (1999) *FEBS Lett.* **447**, 5–9.
26. Grier, J. D., Yan, W. & Lozano, G. (2002) *Genesis* **32**, 145–147.
27. Grier, J. D., Xiong, S., Elizondo-Fraire, A. C., Parant, J. M. & Lozano, G. (2006) *Mol. Cell. Biol.* **26**, 192–198.
28. Herzog, K. H., Chong, M. J., Kapsetaki, M., Morgan, J. I. & McKinnon, P. J. (1998) *Science* **280**, 1089–1091.
29. O'Rourke, N. A., Sullivan, D. P., Kaznowski, C. E., Jacobs, A. A. & McConnell, S. K. (1995) *Development (Cambridge, U.K.)* **121**, 2165–2176.
30. Noctor, S. C., Martinez-Cerdeno, V., Ivic, L. & Kriegstein, A. R. (2004) *Nat. Neurosci.* **7**, 136–144.
31. de Oca Luna, R. M., Tabor, A. D., Eberspaecher, H., Hulboj, D. L., Worth, L. L., Colman, M. S., Finlay, C. A. & Lozano, G. (1996) *Genomics* **33**, 352–357.
32. Leveillard, T., Gorry, P., Niederreither, K. & Wasylyk, B. (1998) *Mech. Dev.* **74**, 189–193.
33. Graus-Porta, D., Blaess, S., Senften, M., Littlewood-Evans, A., Damsky, C., Huang, Z., Orban, P., Klein, R., Schittny, J. C. & Muller, U. (2001) *Neuron* **31**, 367–379.
34. Soriano, P. (1999) *Nat. Genet.* **21**, 70–71.
35. Stad, R., Ramos, Y. F., Little, N., Grivell, S., Attema, J., van Der Eb, A. J. & Jochemsen, A. G. (2000) *J. Biol. Chem.* **275**, 28039–28044.
36. de Rozieres, S., Maya, R., Oren, M. & Lozano, G. (2000) *Oncogene* **19**, 1691–1697.
37. Linares, L. K., Hengstermann, A., Ciechanover, A., Muller, S. & Scheffner, M. (2003) *Proc. Natl. Acad. Sci. USA* **100**, 12009–12014.
38. de Graaf, P., Little, N. A., Ramos, Y. F., Meulmeester, E., Letteboer, S. J. & Jochemsen, A. G. (2003) *J. Biol. Chem.* **278**, 38315–38324.
39. Pan, Y. & Chen, J. (2003) *Mol. Cell. Biol.* **23**, 5113–5121.
40. Liu, G., Parant, J. M., Lang, G., Chau, P., Chavez-Reyes, A., El-Naggar, A. K., Multani, A., Chang, S. & Lozano, G. (2004) *Nat. Genet.* **36**, 63–68.
41. Carroll, P. M., Tsirka, S. E., Richards, W. G., Frohman, M. A. & Strickland, S. (1994) *Development (Cambridge, U.K.)* **120**, 3173–3183.
42. Bruins, W., Zwart, E., Attardi, L. D., Iwakuma, T., Hoogvorst, E. M., Beems, R. B., Miranda, B., van Oostrom, C. T., van den Berg, J., van den Aardweg, G. J., et al. (2004) *Mol. Cell. Biol.* **24**, 8884–8894.
43. Wu, W. S., Heinrichs, S., Xu, D., Garrison, S. P., Zambetti, G. P., Adams, J. M. & Look, A. T. (2005) *Cell* **123**, 641–653.